Distinct functions for Rho1 in maintaining adherens junctions and apical tension in remodeling epithelia

Stephen J. Warner[1,2] and Gregory D. Longmore[1,2]

[1]Department of Medicine and [2]Department of Cell Biology and Physiology, Washington University, St. Louis, MO 63110

Maintenance and remodeling of adherens junctions (AJs) and cell shape in epithelia are necessary for the development of functional epithelia and are commonly altered during cancer progression/metastasis. Although formation of nascent AJs has received much attention, whether shared mechanisms are responsible for the maintenance and remodeling of AJs in dynamic epithelia, particularly in vivo, is not clear. Using clonal analysis in the postmitotic *Drosophila melanogaster* pupal eye epithelium, we demonstrate that Rho1 is required to maintain AJ integrity independent of its role in sustaining apical cell tension. Rho1 depletion in a remodeling postmitotic epithelium disrupts AJs but only when depleted in adjacent cells. Surprisingly, neither of the Rho effectors, Rok or Dia, is necessary downstream of Rho1 to maintain AJs; instead, Rho1 maintains AJs by inhibiting *Drosophila* epithelial cadherin endocytosis in a Cdc42/Par6-dependent manner. In contrast, depletion of Rho1 in single cells decreases apical tension, and Rok and myosin are necessary, while Dia function also contributes, downstream of Rho1 to sustain apical cell tension.

Introduction

A hallmark of epithelia is the presence of intercellular junctions. The two apical-most junctions are tight junctions and adherens junctions (AJs). AJs mediate adhesion between cells and, by coupling to the actomyosin cytoskeleton, provide for tension within epithelial sheets or between cells. The core component of AJs is epithelial cadherin (E-cadherin), and proper localization and function of E-cadherin is critical for the development and morphogenesis of metazoans and maintenance of adult epithelia (Gumbiner, 2005).

Distinct E-cadherin adhesive functions are required during the formation and stabilization of newly forming or nascent AJs, as opposed to maintenance and remodeling of formed AJs (Capaldo and Macara, 2007). The former process has been extensively characterized using cell biological systems such as MDCK epithelial cells, in which the formation of nascent AJs can occur between two single cells (Adams et al., 1998) or within a monolayer of cells in response to calcium (Gumbiner et al., 1988), and developmental systems such as *Drosophila melanogaster* embryogenesis, in which dorsal closure brings two epithelial sheets together to form nascent AJs (Jacinto et al., 2002). A less well-understood process, in general, is the maintenance and remodeling of formed AJs as occurs in some adult tissue epithelium or during developmental morphogenesis. Adult, fully differentiated epithelia such as those present in skin and intestine have stem cells that constantly replenish older epithelial cells as they are shed. To do so, these new epithelial cells need to remodel their junctions so as to migrate yet maintain junctions such that the epithelium remains intact and functional (Hollande et al., 2005; Niessen, 2007). Pathologically, misregulation and turnover of mature epithelial AJs are associated with cancer metastasis (D'Souza-Schorey, 2005). Thus, determining how AJs in epithelia are maintained and remodeled will have important implications for epithelial morphogenesis during development, adult tissue homeostasis, and disease states.

Rho GTPases are molecular switches that regulate epithelial cell cytoskeletal dynamics and cell–cell adhesion (Braga et al., 1997; Takaishi et al., 1997; Harden et al., 1999; Yamada and Nelson, 2007). To do so, active Rho proteins associate with effector proteins that mediate downstream signaling events to control specific cell responses. The ability of Rho proteins to activate different

Correspondence to Gregory D. Longmore: glongmor@dom.wustl.edu

Abbreviations used in this paper: AJ, adherens junction; APF, after puparium formation; CA, constitutively active; Cor, Coracle; Daam, Dishevelled-associated activator of morphogenesis; DE-cadherin, *Drosophila* E-cadherin; Dlg, Discs large; DN, dominant negative; E-cadherin, epithelial cadherin; GMR, glass multimer reporter; hsFLP, heat shock flippase; LOF, loss-of-function; MARCM, mosaic analysis with a repressible cell marker; MLC, myosin light chain; PEC, pigment epithelial cell; SJ, septate junction; UAS, upstream activation sequence.

© 2009 Warner and Longmore This article is distributed under the terms of an Attribution–Noncommercial–Share Alike–No Mirror Sites license for the first six months after the publication date (see http://www.jcb.org/misc/terms.shtml). After six months it is available under a Creative Commons License (Attribution–Noncommercial–Share Alike 3.0 Unported license, as described at http://creativecommons.org/licenses/by-nc-sa/3.0/).

The Rockefeller University Press $30.00
J. Cell Biol. Vol. 185 No. 6 1111–1125
www.jcb.org/cgi/doi/10.1083/jcb.200901029

THE JOURNAL OF CELL BIOLOGY

Downloaded from http://rupress.org/jcb/article-pdf/185/6/1111/1899046/jcb_200901029.pdf by guest on 05 December 2025

effectors is believed to be responsible for their functional diversity (Bishop and Hall, 2000), yet whether certain effectors can be assigned to specific roles and what those roles are, especially in vivo, are still uncertain.

In mammals, the Rho subfamily of Rho GTPases consists of three members, RhoA, RhoB, and RhoC. All three members are expressed ubiquitously (Wennerberg and Der, 2004), bind similar downstream effectors, including ROCK1/2 and mammalian Dia1/2 (Wheeler and Ridley, 2004), and share similar functions such as promoting stress fiber formation and adhesion maturation (Vega and Ridley, 2007). However, differences also exist. RhoB may have unique functions in endosome transport, whereas RhoA and RhoC are more involved in generating actomyosin tension (Wheeler and Ridley, 2004). Because the common use of dominant mutant proteins likely affects more than one Rho protein, attempts have been made to uncover functional differences between Rho proteins by generating gene-specific mouse knockouts. The mouse knockout of RhoA is embryonic lethal (Wang and Zheng, 2007), whereas knockouts of RhoB (Liu et al., 2001) and RhoC (Hakem et al., 2005) develop normally. Thus, the presence of multiple members of Rho in mammals has complicated the precise determination of their functions in vivo. In contrast, in *Drosophila*, only one Rho member exists, Rho1, and studies in *Drosophila* have made significant contributions in determining Rho1's function in the development of several different tissues (for review see Johndrow et al., 2004). In addition, several of the Rho effectors, including Rok (*Drosophila* ROCK) and Dia, have only one member in *Drosophila*, allowing for a more straightforward analysis of the specific contributions of these effectors to Rho function in vivo.

The *Drosophila* pupal eye is a postmitotic monolayer neuroepithelium that has been a useful model system in which to study epithelial morphogenesis (Tepass and Harris, 2007). It is composed of ∼800 repeating units called ommatidia. Each ommatidium is composed of four cell types: eight photoreceptors, four glial-like cone cells, three mechanosensory bristles, and eleven pigment epithelial cells (PECs). Between 18 and 41 h after puparium formation (APF), PECs undergo patterning into a hexagonal array that surrounds and optically insulates the neuronal core of each ommatidium (Cagan and Ready, 1989). During this morphogenic/maturation process, PECs remodel their AJs as cells reposition themselves relative to one another to achieve their proper niche and form the tissue architecture (Bao and Cagan, 2005; Larson et al., 2008). Concurrently, to preserve the integrity of the epithelium, PECs maintain their AJs. The final result is a predictable repeating pattern with high fidelity of mature epithelial cells with distinct cell shapes and AJs. We used the epithelium of the *Drosophila* pupal eye to ask whether and how the in vivo functions of Rho1 and its two main downstream effectors, Rok and Dia, affect remodeling of formed AJs, as opposed to Rho1's role in the formation/stabilization of new AJs.

Results

Global depletion of Rho1 in a formed epithelium disrupts AJs

To determine whether and how Rho1 influences the maintenance of a remodeling epithelium in vivo, we genetically decreased Rho1 throughout the *Drosophila* pupal eye. Because null alleles of *Rho1* are homozygous lethal before pupal development, we generated GAL4-inducible RNAi transgenic lines targeting *Rho1*. Two RNAi lines, upstream activation sequence (UAS)–Rho1-RNAi1 and UAS-Rho1-RNAi2, produced similar phenotypes when expressed in the pupal eye, and UAS-Rho1-RNAi1 (referred to as Rho1-RNAi) was used for the rest of the study as it produced the stronger phenotype.

By 41 h APF, the PECs of the pupal eye are fully patterned and begin to undergo the final stages of differentiation (Fig. 1, a and b). Expression of Rho1-RNAi throughout the pupal eye beginning at puparium formation (0 h APF), using the eye-specific promoter *glass multimer reporter* (*GMR*)*–gal4*, resulted in severe disruptions of AJs, as detected by immunostaining for *Drosophila* E-cadherin (DE-cadherin), Armadillo (*Drosophila* β-catenin), and α-catenin at 41 h APF (Fig. 1, c and d). Interestingly, only AJs between PECs were affected, whereas AJs between a PEC and cone cell or between cone cells were not (Fig. 1 d″) despite equivalent expression of Rho1 in PECs and cone cells (Fig. S1 d) and equivalent RNAi depletion in both cell types (Fig. S1, d and e). The ability of Rho1-RNAi to decrease expression of Rho1 was confirmed by immunofluorescence of larval wing discs, Western blotting of pupal eyes at 41 h APF, and immunofluorescence of pupal eyes at 21 and 41 h APF (Fig. S1). To demonstrate phenotypic specificity, coexpression of Rho1 with Rho1-RNAi reverted pupal eyes to wild type (Fig. S1 c), whereas overexpression of closely related Cdc42 or Rac1 did not (not depicted). Finally, Rho1-RNAi phenotypes were enhanced in *Rho1*-null heterozygous backgrounds, with either a deficiency deleting *Rho1* or *Rho1*-null alleles (Fig. S2, a–f). Because only a residual amount of Rho1 protein remains in pupal eyes expressing Rho1-RNAi (Fig. S1), removing a genomic copy of Rho1 may enhance the phenotype by decreasing the levels of Rho1 below a critical threshold earlier in development.

To determine when expression of the Rho1-RNAi, and thus depleted levels of Rho1, began to disrupt AJs in pupal eye development, we used live imaging of pupal eyes expressing Rho1-RNAi and α-catenin–GFP to label AJs (Larson et al., 2008). In control wild-type pupal eyes between 20 and 28 h APF, AJs are maintained between PECs (Video 1). When Rho1-RNAi was expressed at puparium formation (0 h APF), AJs were intact at 20 h APF and then gradually became disrupted starting at 21 h APF (Videos 2 and 3). This suggested that Rho1 regulated AJs beginning at 21 h APF.

Depletion of Rho1 in adjacent cells is required to disrupt AJs, whereas decreased apical tension is cell autonomous

To determine whether AJ regulation by Rho1 was cell autonomous, clones of PECs expressing Rho1-RNAi were generated using the flippase-out technique (Ito et al., 1997). Surprisingly, depleting Rho1 in a single PEC did not affect AJs (Fig. 2 a) or the polarized localization of DE-cadherin (Fig. 2 c) but did result in enlarged apical cell area (Fig. 2, a and c; and Table S1). However, in multiple-cell Rho1-RNAi clones, AJs were disrupted but only between adjacent clonal cells and not between wild-type and clonal cells (Fig. 2 b). Enlarged apical area was present in all

Downloaded from http://rupress.org/jcb/article-pdf/185/6/1111/1899046/jcb_200901029.pdf by guest on 05 December 2025

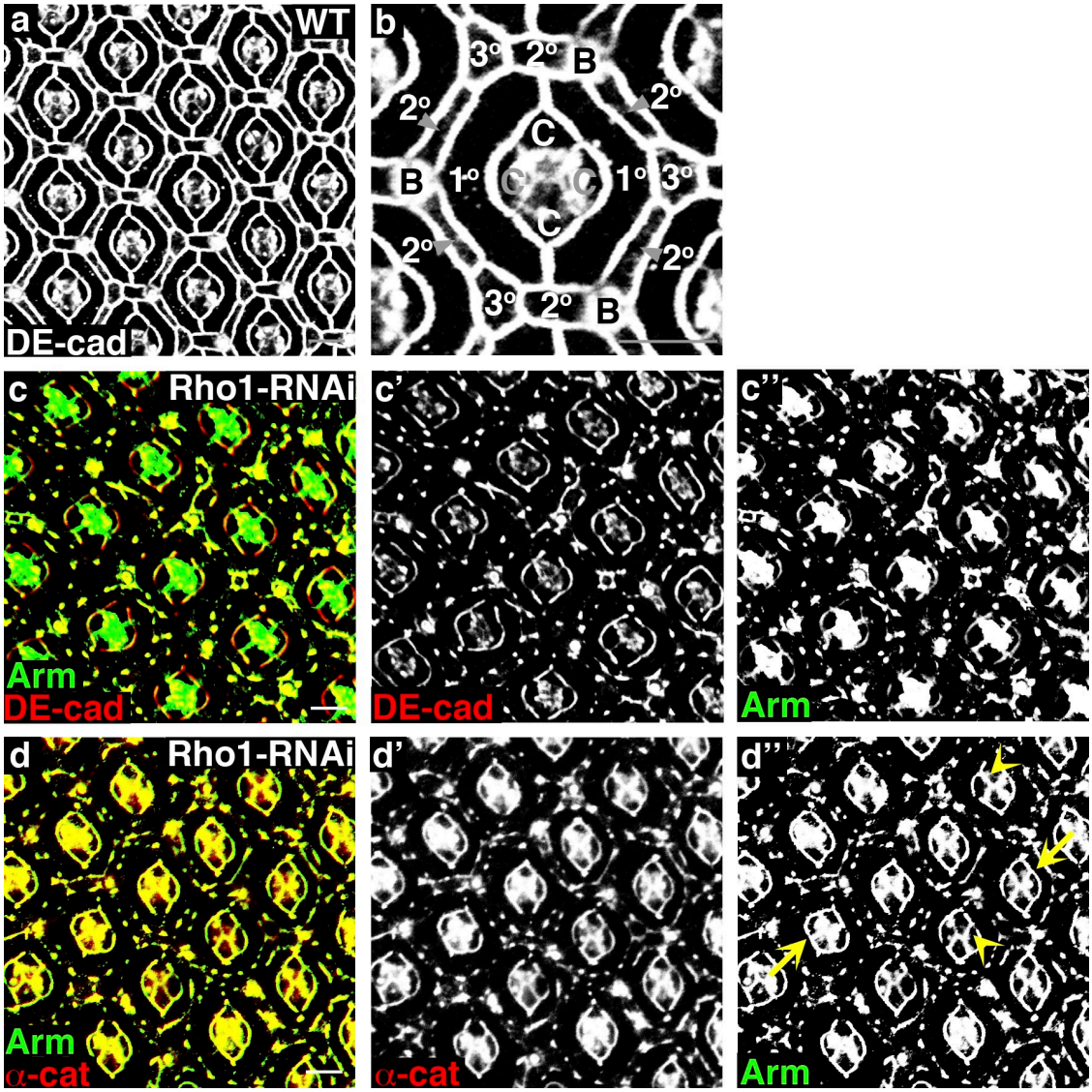

Figure 1. **Rho1 is required to maintain AJs in the pupal eye.** (a and b) Confocal immunofluorescent localization of DE-cadherin (DE-cad) in wild-type pupal eye. B, bristle bell; C, cone cell; 1°, primary PEC; 2°, secondary PEC; 3°, tertiary PEC. The photoreceptors are basal to this optical section. Anterior is to the right in all images. This and subsequent pupal eyes are shown at 41 h APF unless otherwise noted. (c and d) Confocal immunofluorescent localization of the AJ components DE-cadherin and Armadillo (Arm; c) and Armadillo and α-catenin (α-cat; d) in the pupal eye expressing Rho1-RNAi using *GMR-gal4* (GMR>Rho1-RNAi). Arrows identify AJs between primary PECs and cone cells, and arrowheads identify AJs between cone cells. Bars, 10 μm.

Rho1-depleted clones regardless of the Rho1 status of neighboring cells (Fig. 2 b). This clonal analysis indicated that a decrease in Rho1 in adjacent cells was necessary to disrupt AJs, whereas the ability of Rho1 to sustain apical cell area was a cell autonomous effect.

To confirm that the observed Rho1-RNAi clonal phenotypes were indeed the result of loss of Rho1 function, we used mosaic analysis with a repressible cell marker (MARCM; Lee and Luo, 1999) to generate clonal cells homozygous for the *Rho1*-null alleles $Rho1^{72F}$ and $Rho1^{72O}$. MARCM clones of $Rho1^{72F}$ and $Rho1^{72O}$ (hereafter referred to as $Rho1^{72}$) resulted in identical phenotypes but more severe than Rho1-RNAi (Fig. 2, d and e; and Table S1) and depletion of Rho1 protein (Fig. 2 d″). F-actin localization at the level of AJs was disrupted in $Rho1^{72}$ clones, which is consistent with Rho1's role in regulation of actin dynamics (Fig. 2 e and Table S2). Furthermore, $Rho1^{72}$ clones were rescued by expressing Rho1 in the clones, and, in some of these Rho1-rescued $Rho1^{72}$ clones, decreased apical area was observed, likely because of high level overexpression of ectopic Rho1 (Fig. 2, f and f″; and Table S1).

Rho1 does not affect septate junction (SJ) organization despite disrupting AJs

In *Drosophila*, the functional homologue of the vertebrate tight junction is the SJ, which, in contrast to vertebrate epithelia, lies basal to the AJs (Furuse and Tsukita, 2006). Having demonstrated that a loss of Rho1 disrupts pupal eye AJs, we asked whether a decrease in Rho1 affected SJs by analyzing the localization of Discs large (Dlg) and Coracle (Cor) in $Rho1^{72}$ MARCM clones. Between two clonal cells, where the AJs were clearly disrupted, Dlg and Cor localization was unaffected (Fig. 3, a and b; and Fig. S2 g). Depletion of Rho1 in the pupal wing, as observed

Downloaded from http://rupress.org/jcb/article-pdf/185/6/1111/1899046/jcb_200901029.pdf by guest on 05 December 2025

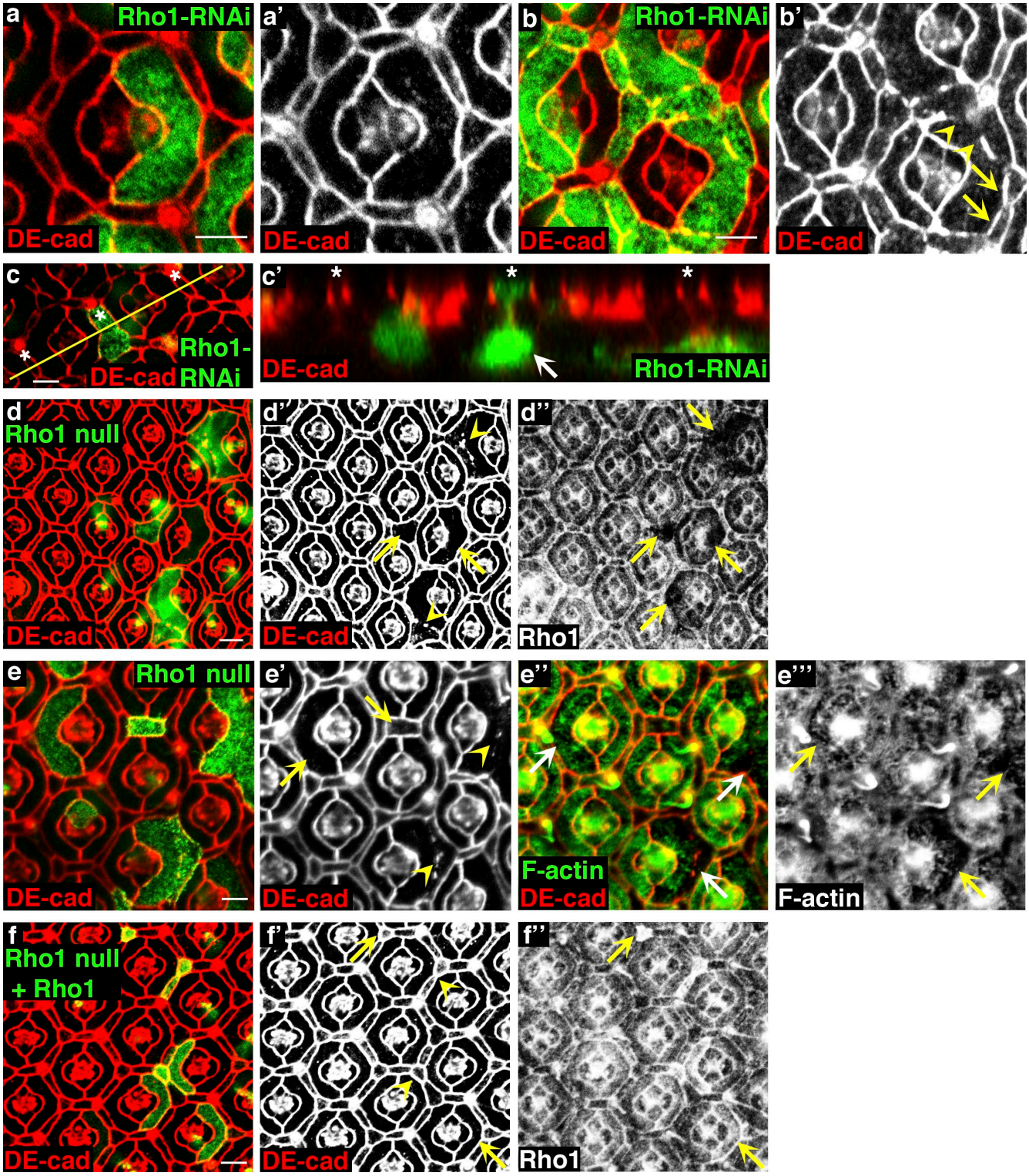

Figure 2. **Depletion of Rho1 in adjacent cells is required to disrupt AJs, but decreased apical tension is cell autonomous.** (a and b) Confocal immunofluorescent localization of DE-cadherin (DE-cad) in a single PEC clone (a and a′) and multiple cell clones (b and b′) expressing Rho1-RNAi (marked with GFP). Arrows in b′ identify intact AJs between a clonal cell and wild-type cell, and arrowheads identify disrupted AJs between two adjacent clonal cells. (c and c′) Apical (c) and lateral (c′) optical sections of DE-cadherin immunofluorescent localization in a Rho1-RNAi clonal cell. The yellow line (c) identifies where the lateral section (c′) was taken. The asterisks mark analogous cells in adjacent ommatidia. The arrow (c′) identifies a Rho1-RNAi clone. (d–d″) Confocal immunofluorescent localization of DE-cadherin (d and d′) and Rho1 (d″) in *Rho1*^{72} (Rho1 null) MARCM clones (clonal cells are GFP positive). (e–e‴) Confocal immunofluorescent localization of DE-cadherin (e–e″) and phalloidin staining (F-actin; e″ and e‴) in *Rho1*^{72} MARCM clones. (d and e) Arrows identify clonal cells, and arrowheads identify disrupted AJs between two clonal cells. (f–f″) Confocal immunofluorescent localization of DE-cadherin (f and f′) and Rho1 (f″) in *Rho1*^{72} MARCM pupal eye clones overexpressing Rho1. Arrows identify cells with rescued apical profiles, and arrowheads identify rescued AJs between clonal cells. Bars, 10 µm.

Downloaded from http://rupress.org/jcb/article-pdf/185/6/1111/1899046/jcb_200901029.pdf by guest on 05 December 2025

in the pupal eye, resulted in increased apical cell areas and disruption of AJs but not SJs (Fig. 3, d and e). To determine whether, in general, AJs can be disrupted without affecting SJs in the pupal eye, we generated MARCM clones with a null allele of *shotgun* (*DE-cadherin*), shg^{R69}. Similar to $Rho1^{72}$ clones, SJs remained intact in shg^{R69} clones (Fig. 3 c). This result is similar to that observed in mammalian MDCK cells in which depletion of E-cadherin in islands of cells with formed junctions did not affect tight junctions (Capaldo and Macara, 2007). Unlike the requirement for depletion of Rho1 in adjacent cells to disrupt AJs, depletion of DE-cadherin in a single cell disrupted AJs around that cell (Fig. 3 c′, arrowhead; and Fig. S2 h).

Rok and myosin are not necessary for the maintenance or remodeling of formed AJs

Active Rho regulates cellular responses through binding to and activating downstream effector proteins/enzymes. Two major effectors of active Rho are the Rho kinases and diaphanous proteins, both of which have only one member in *Drosophila*. Rok is a serine/threonine kinase that activates the myosin light chain (MLC), leading to increased myosin activity and actomyosin contractility (Conti and Adelstein, 2008).

To determine the role of the Rho1–Rok–myosin axis in mature pupal eye epithelium morphogenesis, MARCM clones of the rok^2-null allele, *spaghetti squash* sqh^{AX3}, a null allele of the *Drosophila* homologue of MLC, and zip^1, a null allele of *Drosophila* myosin heavy chain *zipper*, were generated. In all instances, single-cell clones had an increased apical cell area similar to $Rho1^{72}$ clones (Fig. 4, a, c, and d; and Table S1). However, in contrast to $Rho1^{72}$ clones, in multiple neighboring null clones, all AJs were completely intact (Fig. 4, b–d). The rok^2 and $Rho1^{72}$ clonal cells exhibited an equivalent decrease of MLC phosphorylation (Fig. S2, i and j; and Table S3), indicating that Rok activity was decreased equally in rok^2 and $Rho1^{72}$ clones. Decreased MLC activity in sqh^{AX3} clones was confirmed by immunofluorescence with a phospho-MLC antibody (Fig. 4 c″). The absence of myosin heavy chain in zip^1 clones was confirmed by immunofluorescence (Fig. 4 d″). These results indicated that the Rho1–Rok–myosin axis was necessary to maintain appropriate apical cell tension but not required to maintain/remodel formed AJs.

Dia is not required to maintain or remodel AJs in vivo but cooperates with Rok to maintain apical cell tension

Another major effector of Rho is the formin protein Dia, which promotes linear F-actin synthesis. In both vertebrate and *Drosophila* cells, it has been shown to be important for nascent AJ formation (Sahai and Marshall, 2002; Kobielak et al., 2004; Carramusa et al., 2007; Homem and Peifer, 2008). Therefore, we asked whether AJ disruption after Rho1 depletion was mediated by decreased Dia activity in remodeling epithelia.

Pupal eye epithelial AJs were unaffected in MARCM clones containing dia^5, a strong hypomorphic allele, despite a significant decrease in Dia protein levels (Fig. 5 a). As this allele was recently found to be temperature sensitive (Homem and Peifer, 2008), we also generated clones that were shifted to the nonpermissive temperature for 30 h before dissection. This also had no affect on AJs organization (Fig. S3 a). Because residual Dia protein remained in the dia^5 clonal cells, we further decreased Dia levels in dia^5 clones by expressing Dia-RNAi in dia^5 MARCM clones. This resulted in essentially undetectable levels of Dia protein in the clonal cells (Fig. 5 b″). Despite this, AJs were still unaffected (Fig. 5 b). In a second approach, we generated clones expressing Dia–constitutively active (CA; Somogyi and Rorth, 2004). When Dia-CA was expressed in adjacent cells, a strengthening of the AJs was not detected (Fig. 5, c and d). As evidence that the Dia-CA protein was active, Dia-CA–expressing cells developed a rounded morphology, especially primary PECs (Fig. 5 c), and had increased intensity of apical F-actin staining (Fig. 5 d). If Dia was acting downstream of Rho1 to regulate mature AJs, expression of Dia-CA in $Rho1^{72}$ MARCM clones should rescue the AJs defect. In $Rho1^{72}$ clones expressing Dia-CA, AJs remained disrupted (Fig. 5 e and Table S4). In sum, these data indicated that Dia was not acting downstream of (i.e., not required for) Rho1 to maintain/remodel formed AJs.

Possibly, the action of both major Rho effectors was required to remodel AJs in formed, remodeling epithelia. To test this possibility, we made clones of cells depleted of both Dia and Rok by expressing Dia-RNAi in rok^2 MARCM clones. Again, mature AJs were not affected in these clones, indicating that Dia and Rok do not cooperate to regulate AJs (Fig. 5 f). Surprisingly, although cells depleted of Dia had no change in apical area (Fig. 5 b and Table S1), expression of Dia-RNAi in rok^2 MARCM clones resulted in a greater increase in apical area compared with rok^2 MARCM clones alone (Figs. 4 b and 5 f and Table S1). These data indicated that Dia and Rok function cooperatively to sustain apical cell tension.

Rho1 regulates AJs through membrane trafficking of DE-cadherin

How then could a loss of Rho1 disrupt mature AJs? To determine whether Rho1 affected DE-cadherin protein levels, we performed Western blot analysis of pupal eyes uniformly expressing Rho1-RNAi at 41 h APF, when Rho1-RNAi caused strong AJ disruptions (Fig. 1 c). The level of DE-cadherin in Rho1-RNAi–expressing tissue relative to control tissue was not significantly different (Fig. 6, a and b). Because Rho1-RNAi expression was driven only in the eye, the decrease in Rho1 protein with the Rho1-RNAi demonstrated that the dissections were specific to the eye tissue (Fig. 6 a).

We also used a genetic approach to address this question. If a loss of Rho1 leads to AJ disruptions strictly because of a decrease in DE-cadherin levels, increasing DE-cadherin in these cells should rescue the AJs. We generated clones that expressed Rho1-RNAi and overexpressed DE-cadherin. Even with high levels of DE-cadherin in cells with decreased Rho1, AJs were still disrupted, as determined by Armadillo localization (Fig. 6 c). To control for the effects of DE-cadherin overexpression on AJs, we generated clones that overexpressed DE-cadherin alone and observed an increased Armadillo localization at the AJ between two clonal cells (Fig. 6 d). Therefore, these results confirmed the Western blot analysis and indicated that the AJ disruptions from decreased Rho1 were not the result of decreased total levels of DE-cadherin in this epithelium.

Membrane trafficking of cadherins is another means by which AJ localization can be regulated (D'Souza-Schorey,

Downloaded from http://rupress.org/jcb/article-pdf/185/6/1111/1899046/jcb_200901029.pdf by guest on 05 December 2025

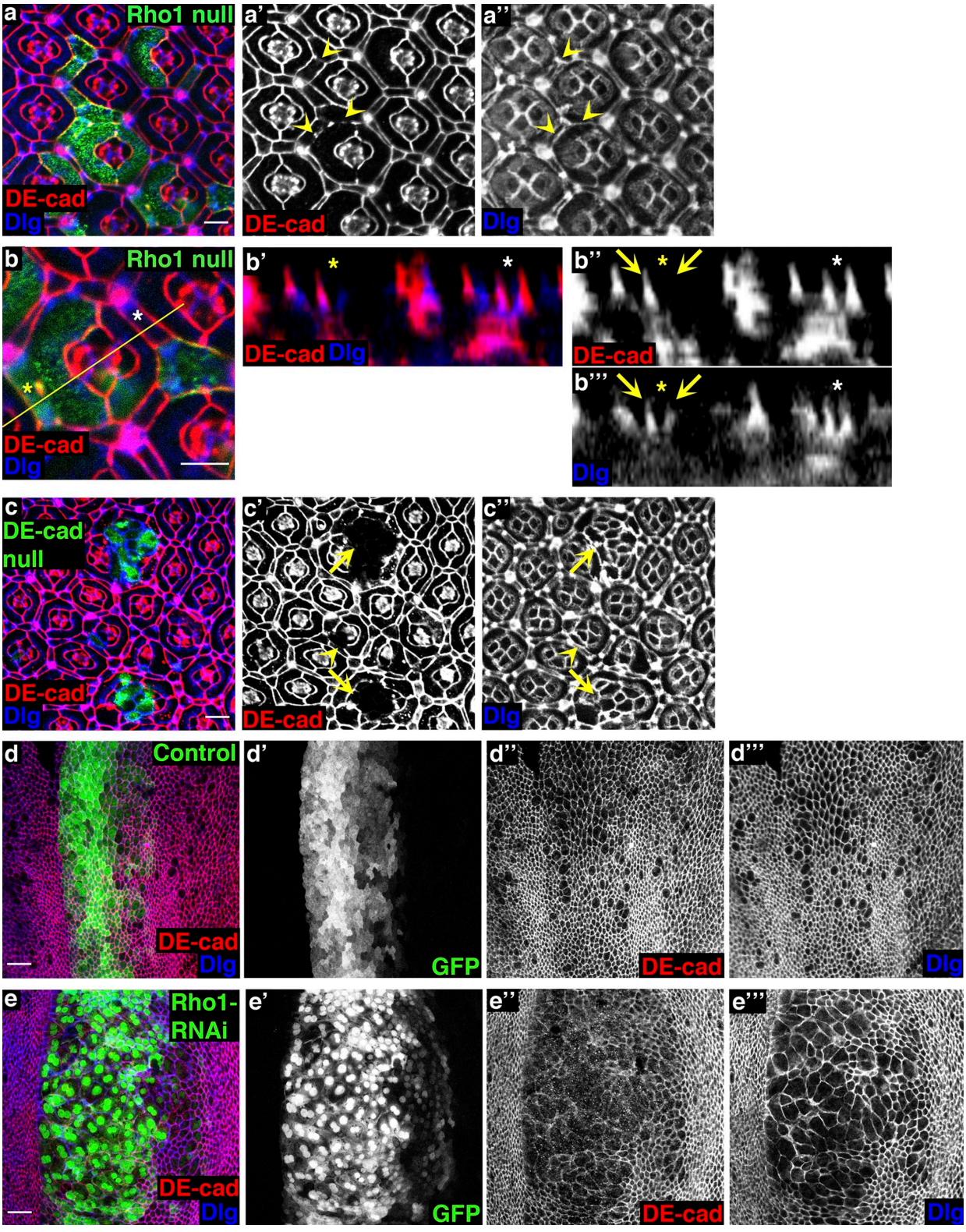

Figure 3. **Rho1 specifically regulates AJs but not SJs in formed, remodeling pupal epithelium.** (a–a″) Confocal immunofluorescent localization of DE-cadherin (DE-cad; a and a′) and Dlg (a and a″) in *Rho1*^{72} MARCM clones. Arrowheads identify AJs (a′) and SJs (a″) between clonal cells. (b–b‴) Confocal immunofluorescent localization of DE-cadherin (b–b″) and Dlg (b, b′, and b‴) in apical (b) and lateral (b′–b‴) optical sections of *Rho1*^{72} MARCM clones. The yellow line (b) identifies where the lateral section (b′–b‴) was taken. The yellow asterisks identify a *Rho1*^{72} MARCM clone, and the white asterisks identify an analogous nonclonal wild-type cell. Arrows identify AJs (b″) and SJs (b‴) of the *Rho1*^{72} clonal cell that neighbors another clonal cell on the right and a nonclonal cell on the left. (c–c″) Confocal immunofluorescent localization of DE-cadherin (c and c′) and Dlg (c and c″) in *shg*^{R69} (DE-cad null) MARCM clones. Arrows identify multiple-cell clones, and arrowheads identify single-cell clones. (d–d‴) Confocal immunofluorescent localization of DE-cadherin (d and d″) and Dlg (d and d‴) in pupal wing epithelial cells expressing GFP using *patched-gal4*. (e–e‴) Confocal immunofluorescent localization of DE-cadherin (e and e″) and Dlg (e and e‴) in pupal wing epithelial cells coexpressing GFP and Rho1-RNAi using *patched-gal4*. Bars, 10 µm.

Downloaded from http://rupress.org/jcb/article-pdf/185/6/1111/1899046/jcb_200901029.pdf by guest on 05 December 2025

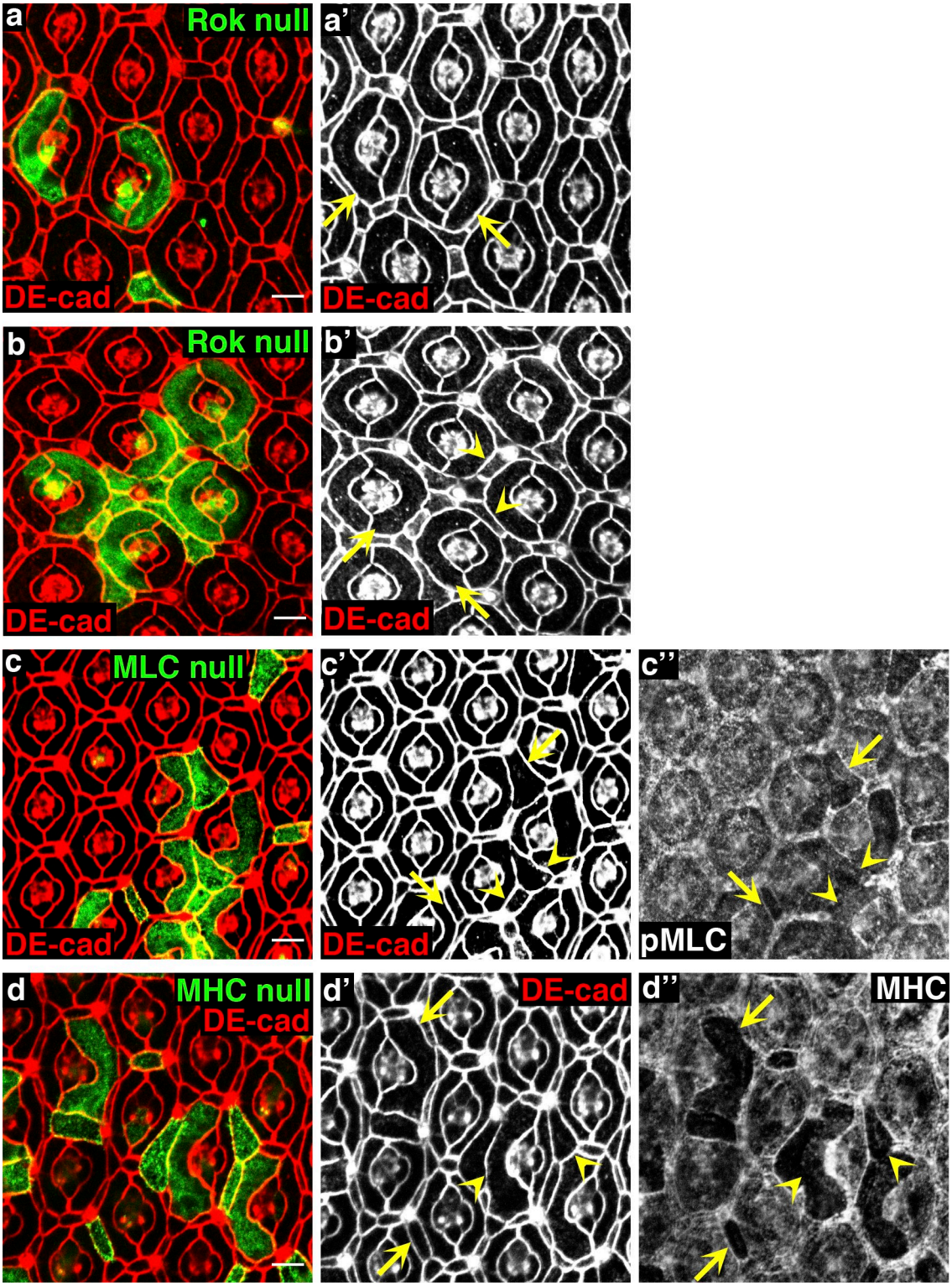

Figure 4. **Rok and myosin are necessary for sustaining apical tension but not maintaining AJs.** (a) Confocal immunofluorescent localization of DE-cadherin (DE-cad) in single-cell *rok*^{2} (Rok null) MARCM clones. (b) Confocal immunofluorescent localization of DE-cadherin in a multiple-cell *rok*^{2} MARCM clone. (c–c″) Confocal immunofluorescent localization of DE-cadherin (c and c′) and phospho-MLC (pMLC; c″) in *sqh*^{AX3} (MLC null) MARCM clones. (d–d″) Confocal immunofluorescent localization of DE-cadherin (d and d′) and Zip (myosin heavy chain [MHC]; d″) in *zip*^{1} (MHC null) MARCM clones. (a–d) Arrows identify clonal cells, and arrowheads identify AJs between clonal cells. Bars, 10 µm.

2005; Yap et al., 2007). E-cadherin has three general trafficking routes: delivery of newly synthesized E-cadherin from the Golgi complex to the plasma membrane, endocytosis and recycling of E-cadherin back to the plasma membrane, and endocytosis of E-cadherin with targeting to the lysosomes for degradation.

Downloaded from http://rupress.org/jcb/article-pdf/185/6/1111/1899046/jcb_200901029.pdf by guest on 05 December 2025

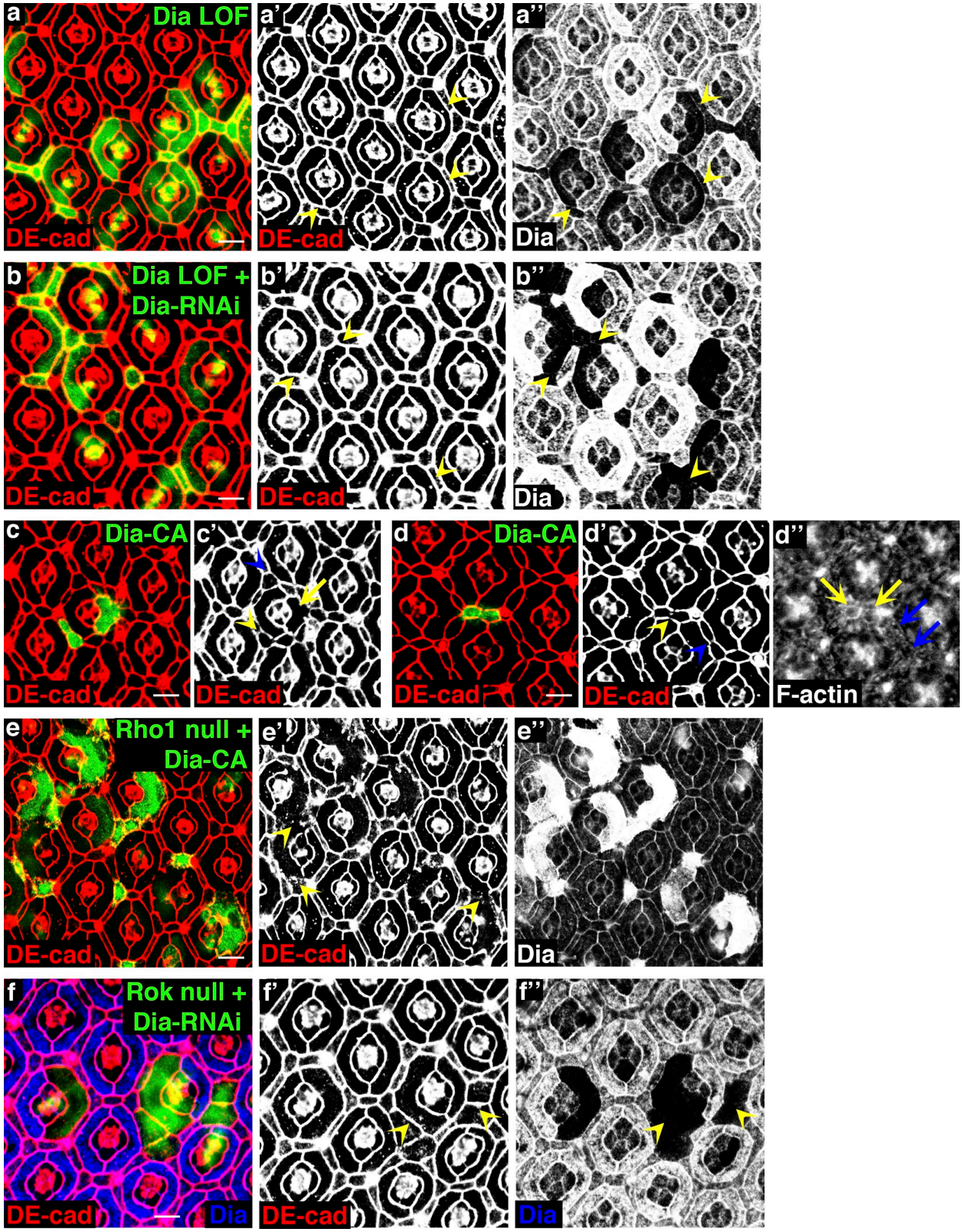

Figure 5. **Dia cooperates with Rok to sustain apical tension but does not maintain formed AJs.** (a–a″) Confocal immunofluorescent localization of DE-cadherin (DE-cad; a and a′) and Dia (a″) in *dia*^{5} (Dia hypomorph/LOF) MARCM clones. (b–b″) Confocal immunofluorescent localization of DE-cadherin (b and b′) and Dia (b″) in *dia*^{5} MARCM clones expressing Dia-RNAi. (c and d) Confocal immunofluorescent localization of DE-cadherin (c–d′) and phalloidin staining (d″) in clones expressing Dia-CA in 38 h APF pupal eyes. Yellow arrows identify clonal cells, whereas blue arrows identify analogous wild-type cells. Yellow arrowheads identify AJs between two clonal cells, whereas blue arrowheads identify AJs between analogous wild-type cells. (e–e″) Confocal immunofluorescent localization of DE-cadherin (e and e′) and Dia (e″) in *Rho1*^{72} MARCM clones expressing Dia-CA. (f–f″) Confocal immunofluorescent localization of DE-cadherin (f and f′) and Dia (f and f″) in *rok*^{2} MARCM clones expressing Dia-RNAi. (a, b, e, and f) Arrowheads identify AJs between two clonal cells. Bars, 10 µm.

Downloaded from http://rupress.org/jcb/article-pdf/185/6/1111/1899046/jcb_200901029.pdf by guest on 05 December 2025

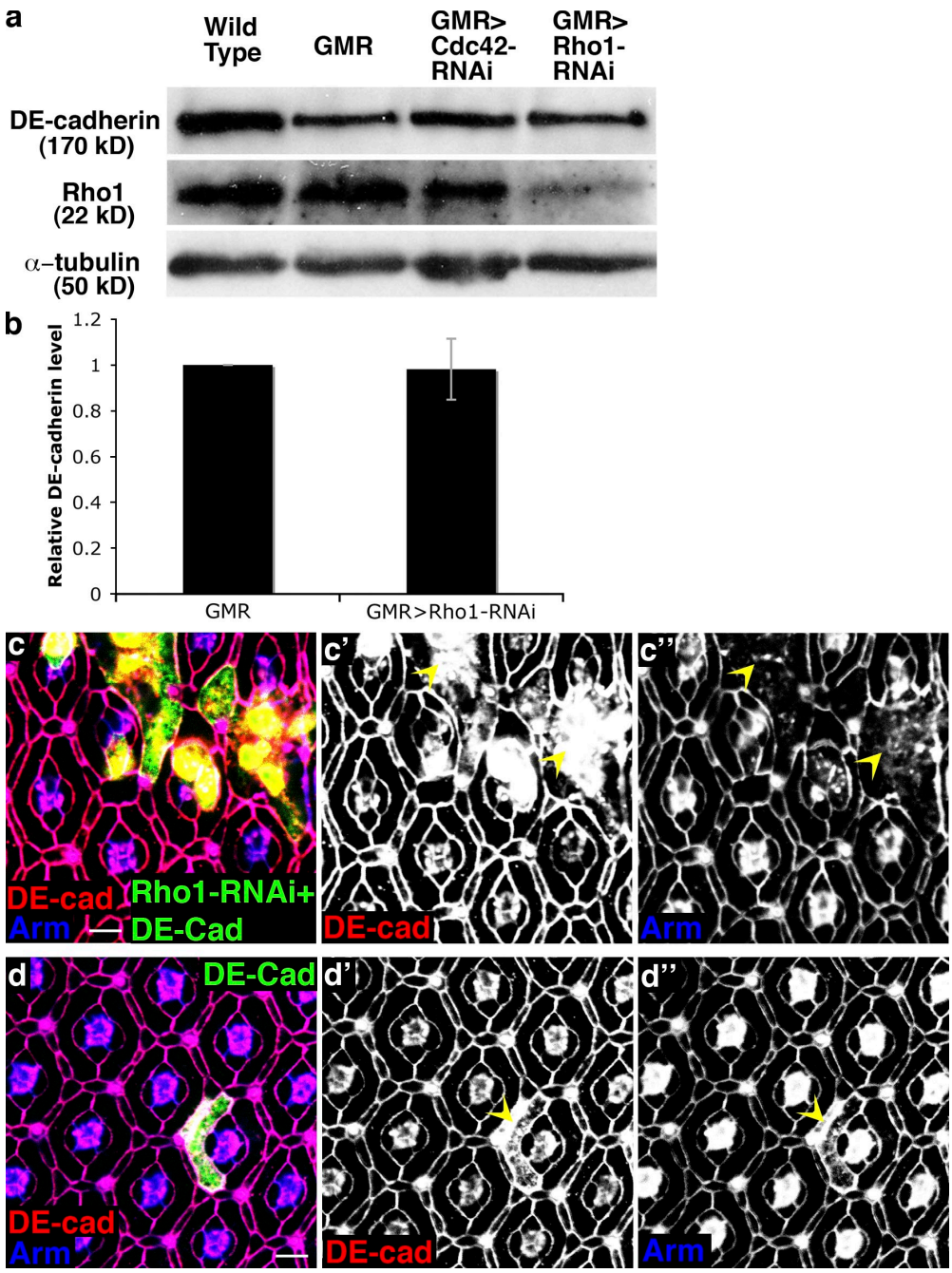

Figure 6. **Rho1 does not maintain formed AJs by regulating total cellular DE-cadherin levels.** (a) Western blot analysis of 41 h APF pupal eyes. (b) Quantification of DE-cadherin levels from control and Rho1-RNAi tissue across two independent experiments. Data are represented as mean ± SD. (c–c″) Confocal immunofluorescent localization of DE-cadherin (DE-cad; c and c′) and Armadillo (Arm; c and c″) in clones coexpressing Rho1-RNAi and DE-cadherin. (d–d″) Confocal immunofluorescent localization of DE-cadherin (d and d′) and Armadillo (d and d″) in a clone overexpressing DE-cadherin alone. (c and d) Arrowheads identify AJs between two clonal cells. Bars, 10 µm.

To determine whether Rho1 controls endocytosis/recycling of DE-cadherin, which involves endocytosis of DE-cadherin into Rab5-containing early endosomes and delivery of DE-cadherin back to the plasma membrane in Rab11-containing recycling endosomes (Yap et al., 2007), we first asked whether blocking endocytosis of DE-cadherin in a Rho1-null clone could rescue the AJ disruption. Expression of a Rab5 dominant-negative (DN) transgene (Rab5-DN; Zhang et al., 2007) or Rab5-RNAi in *Rho1*^{72} clones each reverted the AJ defect seen between two *Rho1*^{72} clonal cells (Fig. 7, c and compare b with a; Fig. S4 a; and Table S4). Importantly, these manipulations had no effect on the decreased apical tension resulting from Rho1 depletion (Fig. 7 b, Fig. S4 a, and Table S5). Clones expressing Rab5-DN or Rab5-RNAi alone did not affect DE-cadherin localization or apical area (Fig. S4, b and c).

In another approach, expression of a CA Rab5 (Rab5-CA; Zhang et al., 2007) in the *Rho1*^{72} clones might be predicted to enhance/worsen the AJ defects in *Rho1*-null adjoining cells.

Downloaded from http://rupress.org/jcb/article-pdf/185/6/1111/1899046/jcb_200901029.pdf by guest on 05 December 2025

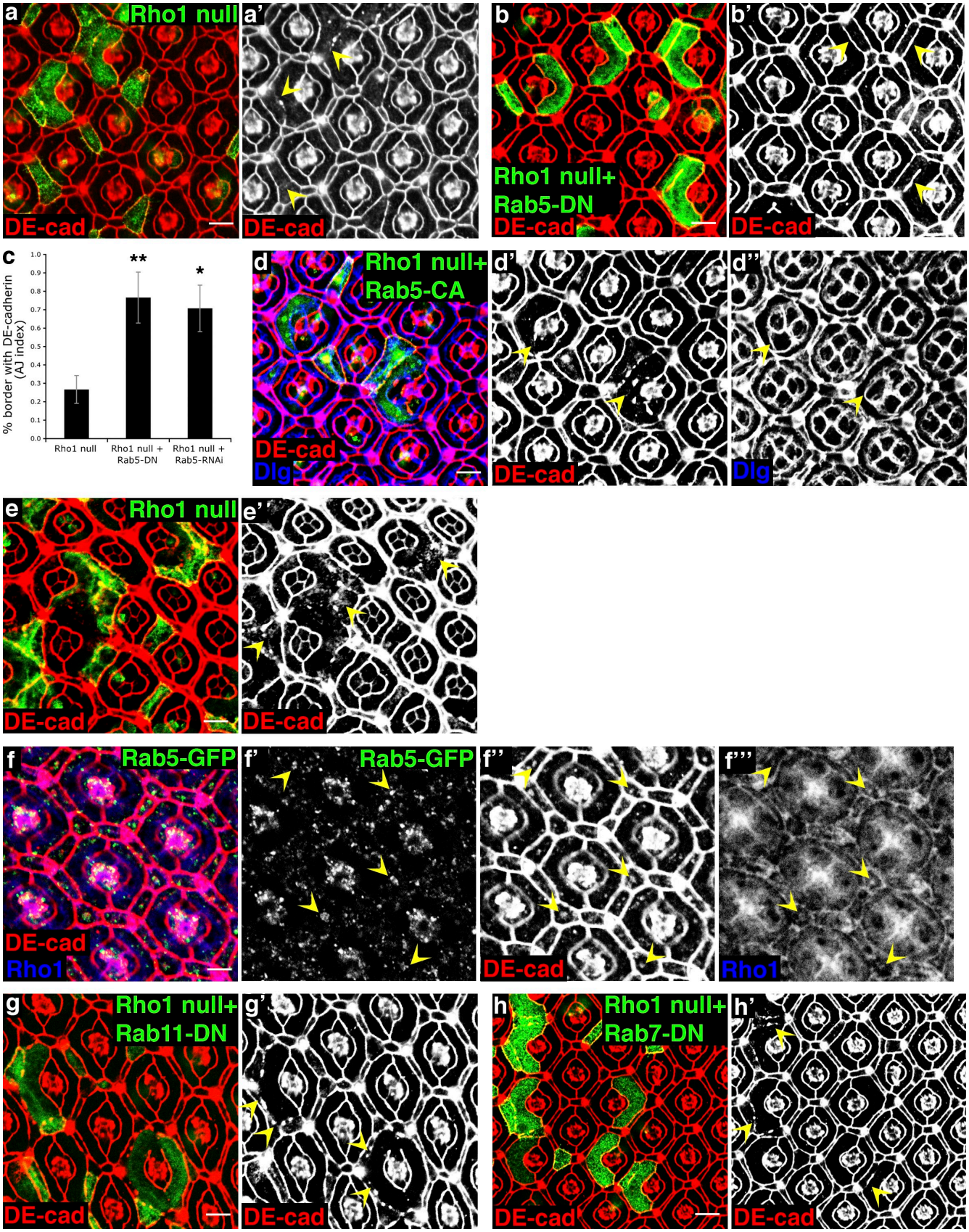

Figure 7. **Rho1 maintains formed AJs by regulating membrane trafficking of DE-cadherin.** (a) Confocal immunofluorescent localization of DE-cadherin (DE-cad) in *Rho1*^{72} MARCM clones. (b) Confocal immunofluorescent localization of DE-cadherin in *Rho1*^{72} MARCM clones expressing Rab5-DN. (a and b) Arrowheads identify AJs between two clonal cells. (c) Quantification of the ratio of border length positive for DE-cadherin immunofluorescence divided by the total border length between two *Rho1*^{72} clonal cells or two *Rho1*^{72} clonal cells expressing Rab5-DN or Rab5-RNAi (AJ index; see Table S4). Data are

Downloaded from http://rupress.org/jcb/article-pdf/185/6/1111/1899046/jcb_200901029.pdf by guest on 05 December 2025

Expression of Rab5-CA in *Rho1*^{72} clones did not worsen the *Rho1*^{72} AJ phenotype between two clonal PECs (Table S4) but did disrupt AJs between a PEC and cone cell, a phenotype which was not observed in *Rho1*^{72} clones (Fig. 7 d). Although clones expressing Rab5-CA alone had increased intracellular DE-cadherin, AJs were unchanged (Fig. S4 d).

If depletion of Rho1 indeed results in increased endocytosis of DE-cadherin (i.e., Rho1 inhibits DE-cadherin endocytosis), Rho1-depleted cells should exhibit increased internalization of DE-cadherin. To detect internalized DE-cadherin, we performed a DE-cadherin endocytosis assay using pupal eyes containing *Rho1*^{72} MARCM clones. *Rho1*^{72} clonal cells had increased intracellular DE-cadherin compared with surrounding wild-type cells (Fig. 7 e), representing increased internalization and/or decreased recycling of DE-cadherin with Rho1 depletion. In addition, pupal eyes expressing Rho1-RNAi had increased intracellular DE-cadherin, much of which colocalized with Rab5, compared with control pupal eyes (Fig. S4, e and f). Consistent with a role for Rho1 in endocytosis of DE-cadherin, Rho1 protein colocalized with Rab5-positive, DE-cadherin–containing endosomes (Fig. 7 f).

To inhibit recycling of internalized endosomes, we expressed Rab11-DN (Zhang et al., 2007) in the *Rho1*^{72} clones. Although *Rho1*^{72} clones exhibit disrupted AJs only between two clonal PECs, expression of Rab11-DN in the *Rho1*^{72} clones led to a worsening of the Rho1-null phenotype. In addition to frequent disruptions of AJs between *Rho1*^{72} clonal cells, disruption of AJs between *Rho1*^{72} clonal cells and wild-type cells was now apparent (Fig. 7 g). The effect of the Rab11-DN on the AJs was specific to the *Rho1*^{72} clones (i.e., loss of Rho1 activity) because neither clones expressing the Rab11-DN alone nor MARCM clones with the *Rab11*^{EP3017} loss-of-function (LOF) allele had affects on the AJs (unpublished data). Rab7-DN (Zhang et al., 2007), which blocks targeting of early endosomes to lysosomes, and Rab8-DN (Zhang et al., 2007), which inhibits transport of vesicles from the Golgi to the plasma membrane, had no effects on the localization of DE-cadherin in *Rho1*^{72} clonal cells (Fig. 7 h and Table S4).

Rho1 regulation of AJs is Cdc42/Par6 dependent

The related GTPase, Cdc42, was recently demonstrated to promote endocytosis and recycling of DE-cadherin in *Drosophila* epithelia (Georgiou et al., 2008; Leibfried et al., 2008). Because cross talk between the activities of Rho GTPase family members is critical for the regulation of many cellular responses such as cell–ECM and cell–cell adhesion and cell migration, we asked whether Rho1 activity limits DE-cadherin trafficking in remodeling pupal epithelium by inhibiting Cdc42. In other words, in the absence of Rho1 (*Rho1*^{72} clones), it is proposed that Cdc42 activity is enhanced and thus E-cadherin endocytosis increased. If so, depletion of Cdc42 in Rho1-null cells could rescue AJ disruptions. To test this, we expressed Cdc42-RNAi in *Rho1*^{72} clones. Like Rab5-DN and Rab5-RNAi, depletion of Cdc42 reverted the AJ defects seen between two *Rho1*^{72} clonal cells (Fig. 8 a and Table S4) but did not affect the increased apical area (Fig. 8 a and Table S5). In another approach to address this question, we asked whether depletion of Cdc42 could rescue the AJ disruptions between two Rho1-RNAi–expressing cells. When Rho1-RNAi was expressed in *Cdc42* LOF clones, AJs between clonal cells remained completely intact (Fig. 8 b), indicating that Cdc42 was required for Rho1 depletion to disrupt AJs. The Cdc42 effector implicated in promoting DE-cadherin endocytosis is Par6 (Georgiou et al., 2008; Leibfried et al., 2008). Expression of Rho1-RNAi in *par6*-null clones had normal-appearing AJs (Fig. 8 c). Cdc42-RNAi, *Cdc42* LOF, or *par6*-null clones alone did not fragment AJs (unpublished data). Together, these data indicate that Rho1 maintained/remodeled AJs in formed epithelia by inhibiting endocytosis and recycling of DE-cadherin in a Cdc42/Par6-dependent manner.

Discussion

We have isolated two specific functions downstream of Rho1 in an in vivo remodeling epithelium, as opposed to formation of nascent cell–cell adhesions. They are to sustain apical cell tension and maintain AJs. The former function is cell autonomous and requires Rok and myosin with a supporting role from Dia, whereas the latter is not cell autonomous and involves inhibition of DE-cadherin endocytosis through Cdc42/Par6, independent of Rok or Dia (Fig. 9). The ability to separate these two phenotypes downstream of Rho is consistent with the idea that Rho proteins achieve their functional diversity by activating several effectors.

Our results showing that Dia has no role in regulating AJs is contrary to several published studies in both mammalian systems (Sahai and Marshall, 2002; Carramusa et al., 2007) and *Drosophila* (Homem and Peifer, 2008). Dia has also been shown to regulate myosin in the control of cell contraction in the *Drosophila* embryo (Homem and Peifer, 2008; Mulinari et al., 2008) and larval eye epithelium (Corrigall et al., 2007). Although we show that Dia cooperates with Rok to regulate apical cell tension, we saw no effect on apical cell shape upon Dia depletion alone in the pupal eye. One explanation for these discrepancies may be inherent differences between mammalian tissue culture systems and in vivo *Drosophila* systems and/or between different stages of *Drosophila* development. Alternatively, although Rok and Dia are necessary for the formation of nascent AJs,

represented as mean ± SD; *, P = 0.000351 for Rho1 null + Rab5-RNAi; **, P = 0.000066 for Rho1 null + Rab5-DN. (d–d″) Confocal immunofluorescent localization of DE-cadherin (d and d′) and Dlg (d and d″) in *Rho1*^{72} MARCM clones expressing Rab5-CA. Arrowheads identify AJ disruptions between PECs and cone cells. (e and e′) Confocal immunofluorescent localization of DE-cadherin after DE-cadherin endocytosis assay in *Rho1*^{72} MARCM clones. Arrowheads identify accumulations of internalized DE-cadherin in Rho1-null clones. (f–f‴) Confocal immunofluorescent localization of DE-cadherin (f and f″) and Rho1 (f and f‴) in the pupal eye expressing Rab5-GFP (f and f′). Arrowheads mark colocalizations between Rab5-GFP, DE-cadherin, and Rho1. This image is 0.75 µm basal compared with other pupal eye images. (g) Confocal immunofluorescent localization of DE-cadherin in *Rho1*^{72} MARCM clones expressing Rab11-DN. Arrowheads identify AJ disruptions between clonal cells and nonclonal cells. (h) Confocal immunofluorescent localization of DE-cadherin in *Rho1*^{72} MARCM clones expressing Rab7-DN. Arrowheads identify AJ disruptions between clonal cells. Bars, 10 µm.

Downloaded from http://rupress.org/jcb/article-pdf/185/6/1111/1899046/jcb_200901029.pdf by guest on 05 December 2025

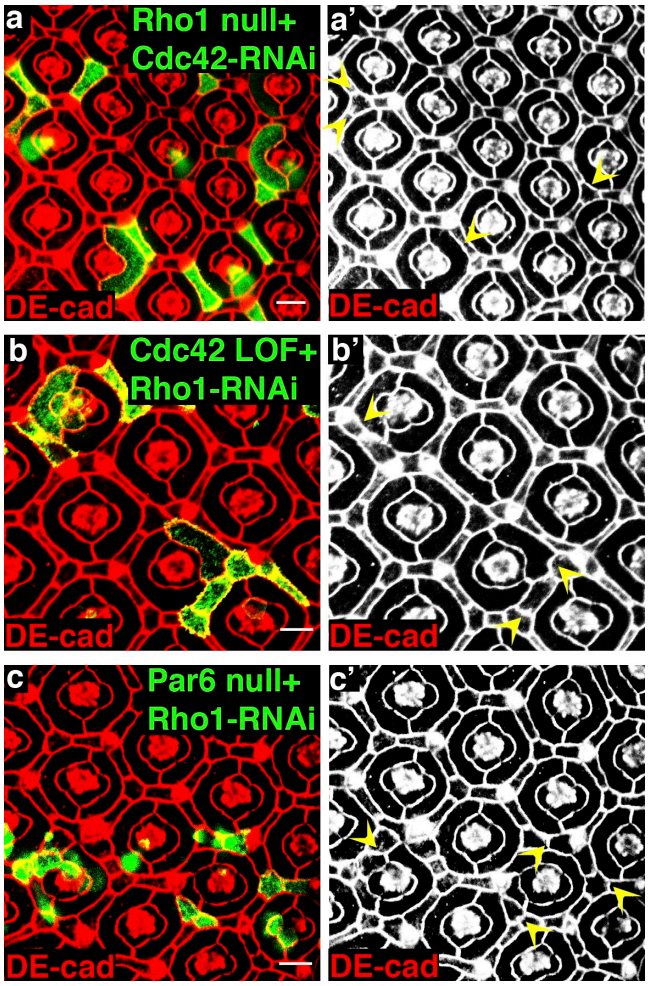

Figure 8. **Rho1 regulation of AJs is Cdc42/Par6 dependent.** (a) Confocal immunofluorescent localization of DE-cadherin (DE-cad) in *Rho1*^{72} MARCM clones expressing Cdc42-RNAi. (b) Confocal immunofluorescent localization of DE-cadherin in *Cdc42*^{4} MARCM clones expressing Rho1-RNAi. (c) Confocal immunofluorescent localization of DE-cadherin in *par6*$^{\Delta 226}$ MARCM clones expressing Rho1-RNAi. (a–c) Arrowheads identify AJs between clonal cells. Bars, 10 µm.

other formin proteins or a combination of different actin nucleating proteins maintains AJs. Another *Drosophila* formin protein that could function with Rho to regulate the actin cytoskeleton is Dishevelled-associated activator of morphogenesis (Daam; Habas et al., 2001; Matusek et al., 2006). However, LOF and gain-of-function experiments showed that Daam, like Dia, did not function to maintain/remodel AJs in pupal epithelium (Fig. S3, b and c).

Our data indicate that Rho affects AJ turnover/remodeling by regulating E-cadherin endocytosis in a Cdc42/Par6-dependent manner. A role for Rho in endocytosis of growth factor receptors in cell lines has been previously reported (Symons and Rusk, 2003; Ridley, 2006) through its effects on actin dynamics. In the Rho1-null pupal eye epithelial clones, we observed a decrease in AJ-associated F-actin intensity; however, Dia-depleted cells (the major Rho actin effector) had unaffected AJs and F-actin intensity (Table S2). Rok can also regulate actin through LIM kinase–Cofilin, but pupal eye Rok-null clones or pupal eyes homozygous for a strong hypomorphic allele of *Drosophila Lim kinase*, *Limk*^{EY08757} (Eaton and Davis, 2005), have intact AJs

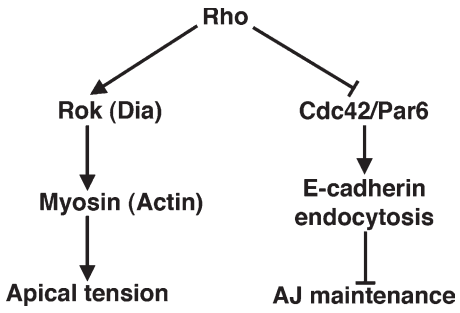

Figure 9. **Working model for Rho function in remodeling, formed epithelia.** Rho regulates apical cell tension and AJs independently. Rho sustains apical cell tension mainly through Rok, but Dia can cooperate with Rok for this role. Rho maintains formed AJs by inhibiting DE-cadherin endocytosis, possibly by inhibiting Cdc42/Par6 activity.

with no decrease in F-actin intensity (Table S2; unpublished data). These data suggest the possibility that Rho1 can regulate actin in a Dia- and Rok-independent manner.

Another possibility is that Rho1 regulates AJ turnover and E-cadherin endocytosis independent of, or in addition to, its effects on actin dynamics. In support of this, we could uncouple disruption of F-actin structures from AJ disruption. Clones with a *chickadee*-null allele (*Drosophila profilin*) have disrupted F-actin and a greater decrease in AJ-associated F-actin than Rho1-null cones (Table S2), yet AJs between Chickadee-null cells are unaffected (Fig. S5 a). Furthermore, an increase in cortical actin in two adjacent cells expressing Dia-CA was not sufficient to affect AJs. Finally, colocalization of Rho1 at DE-cadherin– and Rab5-positive endosomes suggests that Rho1 may be directly involved in endocytosis/recycling of DE-cadherin. Although another Rho effector, PKN, has been implicated in vesicular transport (Mukai, 2003), expression of PKN-RNAi in the pupal eye did not disrupt AJs despite disruption of cell patterning in a manner as or more severe than expression of Rho1-RNAi (Fig. S5 b).

AJs were disrupted after Rho1 depletion only when two adjacent cells were depleted. Although the mechanism behind this is still largely unknown, some insight may be gleaned from the effects of expressing Rab11-DN in the Rho1-null clones, which resulted in disrupted AJs between clonal and nonclonal cells. Perhaps Rab11-recycling endosomes compensate for increased endocytosis of DE-cadherin in the Rho1-depleted cell. If so, this raises the possibility that Rho1 depletion stimulates recycling of Rab11 endosomes. Also, the maintenance of AJs between wild-type and Rho1-null cells is distinct from the loss of AJs between wild-type and DE-cadherin–null cells. In the absence of Rho1, newly synthesized DE-cadherin localizes to the membrane, but its regulation via endocytosis and recycling is altered. Between wild-type and Rho1-null cells, binding in trans to DE-cadherin in the wild-type cell could stabilize DE-cadherin delivered to the membrane of the Rho1-null cell and prevent/limit its endocytosis/recycling. In contrast, between two Rho1-null cells, the altered endocytosis/recycling of DE-cadherin in both cells results in loss of AJ maintenance.

Depletion of Cdc42 or Par6 rescued the AJ defects from Rho1 depletion, suggesting that the effect of Rho1 depletion on AJs involves Cdc42/Par6-dependent regulation of DE-cadherin

Downloaded from http://rupress.org/jcb/article-pdf/185/6/1111/1899046/jcb_200901029.pdf by guest on 05 December 2025

trafficking. Cdc42 and Par6 have recently been implicated in the regulation of DE-cadherin endocytosis and recycling (Georgiou et al., 2008; Harris and Tepass, 2008; Leibfried et al., 2008) but by distinct mechanisms and in different tissues. Georgiou et al. (2008) and Leibfried at al. (2008) both propose a role for Cdc42/Par6 in promoting DE-cadherin endocytosis in pupal notum epithelium, whereas Harris and Tepass (2008) suggest that Cdc42/Par6 regulates DE-cadherin trafficking indirectly by preventing Crumbs endocytosis in embryonic ventral neuroectoderm. Our data are consistent with the former results based on two points. First, both Cdc42-RNAi and Rab5-DN/Rab5-RNAi rescue the Rho1 AJ phenotype, supporting the notion that Cdc42 functions similar to Rab5 and promotes DE-cadherin endocytosis. Second, between two Rho1-null cells, in which DE-cadherin is disrupted, Crumbs either colocalizes with fragmented DE-cadherin or is undisrupted (Fig. S5 c). In contrast, when DE-cadherin–null cells were analyzed, most clones exhibited disrupted Crumbs localization (Fig. S5 d). This suggests that the primary defect from Rho1 depletion is AJ disruption, which likely then affects Crumbs localization, and that the proposed increase in Cdc42 activity resulting from Rho1 depletion is not acting through Crumbs to affect AJs. Although our results are consistent with Georgiou et al. (2008) and Leibfried at al. (2008), the results from Harris and Tepass (2008) may reflect differences in the nature of the ventral neuroectoderm, which has distinct properties even from the dorsal neuroectoderm. Determining how Rho1 regulates Cdc42 activity to maintain AJs and whether Rho1 maintains AJs through Cdc42 in systems other than the pupal eye are important questions for future studies.

Materials and methods

Drosophila stocks

All crosses and staging were performed at 25°C unless otherwise noted. w^{1118} or Canton-S was used as wild type. Stocks are described in FlyBase (http://flybase.bio.indiana.edu). *GMR-gal4*, *tubulin-gal80^{ts}*, *Rho1^{72F}*, *Rho1^{72O}*, *rok^{2}* FRT19A, *dia^{5}* FRT40A, *Cdc42^{4}* FRT19A, UAS-Rho1, UAS-GFP, UAS–Rab5-DN, UAS–Rab5-CA, UAS–Rab11-DN, UAS–Rab7-DN, UAS–Rab8-DN, and *chic^{221}* were provided by the Bloomington Drosophila Stock Center; *patched-gal4*, UAS–DE-cadherin, *wsp^{3}* FRT82B, and *shg^{R69}* FRT42D were provided by R. Cagan (Mount Sinai Medical Center, New York, NY); UAS–Dia-CA was provided by M. Peifer (University of North Carolina at Chapel Hill, Chapel Hill, NC); *zip^{1}* FRT42D was provided by T. Wolff (Washington University, St. Louis, MO); *sqh^{AX3}* was provided by R. Karess (Centre National de la Recherche Scientifique, Gif-sur-Yvette, France); *Daam^{Ex68}* FRT19A and UAS-Daam-CA were provided by J. Mihály (Hungarian Academy of Sciences, Szeged, Hungary); UAS-Rok–catalytic domain was provided by G.-C. Chen (Academia Sinica, Taipei, Taiwan); UAS–Dia-RNAi and UAS–Rab5-RNAi were provided by the Vienna Drosophila RNAi Center; *Rab11^{EP3017}* FRT82B was provided by D. Ready (Purdue University, West Lafayette, IN); UAS-Rab5-GFP was provided by M. González-Gaitán (University of Geneva, Geneva, Switzerland); *parĠ^{Δ226}* FRT19A was provided by C. Doe (University of Oregon, Eugene, OR); and UAS-PKN-RNAi was provided by the National Institute of Genetics.

Rho1-RNAi and Cdc42-RNAi lines were generated as previously described (Bao and Cagan, 2006) using fragments of *Rho1* and *Cdc42* amplified from Canton-S cDNA, respectively. UAS-Rho1-RNAi1 targets 325–786 bp, and UAS-Rho1-RNAi2 targets 770–1310 bp after the start codon of *Rho1*. UAS–Cdc42-RNAi targets the region 191 bp before to 278 bp after the start codon of *Cdc42*.

Clonal analysis and genetics

To generate flippase-out clones overexpressing a transgene, progeny from Act5C>y^{+}>gal4, UAS-GFP; heat shock flippase (hsFLP) crossed to the following genotypes were heat shocked for 30 min at 37°C as third instar larvae or early pupae: (a) UAS-Rho1-RNAi/SM6a-TM6b, (b) UAS–Dia-CA, (c) UAS-Daam-CA, (d) UAS-Rho1-RNAi; UAS–DE-cadherin/SM6a-TM6b, (e) UAS–DE-cadherin, (f) UAS–Rab5-DN, (g) UAS–Rab5-RNAi, (h) UAS–Rab5-CA, and (i) UAS–Rab11-DN. Clones were marked by the presence of GFP.

MARCM clones were generated by heat shocking third instar larvae with the following genotypes for 1 h at 37°C: (a) hsFLP, UAS-GFP; *Rho1^{72O}*, FRT42D/*tub-gal80*, FRT42D; *tub-gal4/+*, (b) hsFLP, UAS-GFP; *Rho1^{72F}*, FRT42D/*tub-gal80*, FRT42D; *tub-gal4/+*, (c) *rok^{2}*, FRT19A/hsFLP, *tub-gal80*, FRT19A; UAS-GFP, UAS-*lacZ*/+; *tub-gal4/+*, (d) *sqh^{AX3}*, FRT19A/hsFLP, *tub-gal80*, FRT19A; UAS-GFP, UAS-*lacZ*/+; *tub-gal4/+*, (e) hsFLP, UAS-GFP; *zip^{1}*, FRT42D/*tub-gal80*, FRT42D; *tub-gal4/+*, (f) hsFLP, UAS-GFP; *dia^{5}*, FRT40A/*tub-gal80*, FRT40A; *tub-gal4/+*, (g) hsFLP, UAS-GFP; *dia^{5}*, FRT40A/*tub-gal80*, FRT40A; *tub-gal4*/UAS-Dia-RNAi, (h) *rok^{2}*, FRT19A/hsFLP, *tub-gal80*, FRT19A; UAS-GFP, UAS-*lacZ*/+; *tub-gal4*/UAS–Dia-RNAi, (i) *Daam^{Ex68}*, FRT19A/hsFLP, *tub-gal80*, FRT19A; UAS-GFP, UAS-*lacZ*/+; *tub-gal4/+*, (j) hsFLP, UAS-GFP; *chic^{221}*, FRT40A/*tub-gal80*, FRT40A; *tub-gal4/+*, (k) hsFLP, UAS-GFP; *Rho1^{72}*, FRT42D/*tub-gal80*, FRT42D; *tub-gal4*/UAS-Rho1, (l) hsFLP, UAS-GFP; *Rho1^{72}*, FRT42D/*tub-gal80*, FRT42D; *tub-gal4*/UAS–Dia-CA, (m) hsFLP, UAS-GFP; *Rho1^{72}*, FRT42D/*tub-gal80*, FRT42D; *tub-gal4*/UAS–Rab5-DN, (n) hsFLP, UAS-GFP; *Rho1^{72}*, FRT42D/*tub-gal80*, FRT42D; *tub-gal4*/UAS–Rab5-RNAi, (o) hsFLP, UAS-GFP; *Rho1^{72}*, FRT42D/*tub-gal80*, FRT42D; *tub-gal4*/UAS–Rab5-CA, (p) hsFLP, UAS-GFP; *Rho1^{72}*, FRT42D/*tub-gal80*, FRT42D; *tub-gal4*/UAS–Rab11-DN, (q) hsFLP, UAS-GFP/UAS–Rab7-DN; *Rho1^{72}*, FRT42D/*tub-gal80*, FRT42D; *tub-gal4/+*, (r) hsFLP, UAS-GFP; *Rho1^{72}*, FRT42D/*tub-gal80*, FRT42D; *tub-gal4*/UAS–Rab8-DN, (s) hsFLP, UAS-GFP/UAS–Cdc42-RNAi; *Rho1^{72}*, FRT42D/*tub-gal80*, FRT42D; *tub-gal4/+*, (t) *Cdc42^{4}*, FRT19A/hsFLP, *tub-gal80*, FRT19A; UAS-GFP, UAS-*lacZ*/UAS-Rho1-RNAi; *tub-gal4/+*, and (u) *parĠ^{Δ226}*, FRT19A/hsFLP, *tub-gal80*, FRT19A; UAS-GFP, UAS-*lacZ*/UAS-Rho1-RNAi; *tub-gal4/+*.

Clones were marked by the presence of GFP. Flippase recombination target sites were recombined onto *Rho1^{72O}* (42D), *Rho1^{72F}* (42D), *sqh^{AX3}* (19A), *chic^{221}* (40A) as previously described (Xu and Rubin, 1993). Expression of either GFP alone or GFP and Rho1-RNAi with *patched-gal4* in the pupal wing was performed by crossing *patched-gal4*, UAS-GFP, *tub-gal80^{ts}*/SM6a-TM6b to *w^{1118}* or UAS-Rho1-RNAi/SM6a-TM6b at 18°C. Progeny were shifted to 29°C 3–4 d after egg laying and dissected at 18 h APF.

Immunofluorescence

Pupal eyes or wings were dissected in PBS, fixed in 4% paraformaldehyde for 45 min, washed once in PBS-T (PBS/0.1% Triton X-100), washed twice in PAXD (PBS containing 1% BSA, 0.3% Triton X-100, and 0.3% deoxycholate), and washed once in PAXDG (PAXD with 5% goat serum), all on ice. The tissue was then incubated overnight at 4°C with primary antibodies diluted in PAXDG, washed three times in PBS-T, and incubated overnight at 4°C with secondary antibodies diluted in PAXDG. After washing twice in PBS-T, the tissue was postfixed in 4% paraformaldehyde for 25 min at room temperature, washed twice in PBS-T, and mounted in Vectashield mounting media (Vector Laboratories). Antibodies used were rat anti–DE-cadherin (1:20), mouse anti-Dlg (1:50), mouse anti-Rho1 (1:20), rat anti–α-catenin (1:50), mouse anti-Armadillo (1:50), mouse anti-Cor (1:20; all from the Developmental Studies Hybridoma Bank), rabbit anti-Zip (1:200; provided by T. Wolff), rat anti-Crumbs (1:500; provided by U. Tepass, University of Toronto, Toronto, Ontario, Canada), rabbit anti-Dia (1:500; provided by S. Wasserman, University of California, San Diego, La Jolla, CA), and rabbit anti–phospho-MLC2 (serine 19; 1:20; Cell Signaling Technology). Rhodamine-phalloidin (1:500; Invitrogen) was added in the primary and secondary antibody incubations to visualize F-actin. Secondary antibodies used were Alexa Fluor 488 and 568 (Invitrogen) and Cy5 (Jackson ImmunoResearch Laboratories). Immunofluorescence was analyzed on a confocal microscope (LSM 510; Carl Zeiss, Inc.) using a Plan-Apochromat 63× NA 1.4 oil objective (Carl Zeiss, Inc.) at room temperature with LSM 510 software (Carl Zeiss, Inc.). Photoshop (Adobe) was used to minimally adjust brightness and contrast to whole images. Live imaging of developing pupal eyes from either *GMR-gal4*, UAS–α-catenin–GFP/+ or *GMR-gal4*, UAS–α-catenin–GFP/UAS-Rho1-RNAi was performed as previously described (Larson et al., 2008) on a microscope (Axioplan2; Carl Zeiss, Inc.) with a Plan-Apochromat 63× NA 1.4 oil objective at room temperature using a charge-coupled device camera (Quantix; Photometrics) and ImagePro Plus 5.1 software (Media Cybernetics).

DE-cadherin endocytosis assay

Pupal eyes containing *Rho1^{72}* clones were dissected and processed essentially as previously described (Le Borgne and Schweisguth, 2003). After dissection, pupal eyes were incubated with anti–DE-cadherin antibodies for 45 min at 25°C and processed for immunofluorescence as described in

Downloaded from http://rupress.org/jcb/article-pdf/185/6/1111/1899046/jcb_200901029.pdf by guest on 05 December 2025

the previous section. The lack of AJ staining in photoreceptors in Fig. 7 g indicated that only surface DE-cadherin was labeled with antibody.

Western blot analysis

Pupal eyes 41 h APF were dissected in PBS and transferred to radioimmunoprecipitation assay buffer on ice. Lysates were run on a 10% SDS–polyacrylamide gel and transferred to nitrocellulose. Antibodies used were rat anti–DE-cadherin (1:100), mouse anti–α-tubulin (1:2,000), mouse anti-Rho1 (1:100), and HRP-conjugated secondaries. Quantification was performed using ImageJ version 1.38 (National Institutes of Health) with standard procedures.

Quantification and statistics

Images were analyzed using ImageJ version 1.38. Apical area indices were calculated as the ratio of a clonal cell apical area divided by an analogous neighboring nonclonal cell apical area. F-actin indices were calculated as the ratio of phalloidin staining pixel intensity in a clonal cell divided by that in an analogous neighboring nonclonal cell. Phospho-MLC indices were calculated as the ratio of phospho-MLC immunofluorescence pixel intensity in a clonal cell divided by that in an analogous neighboring nonclonal cell. AJ indices were calculated as the ratio of the border length positive for DE-cadherin immunofluorescence divided by the total border length between two clonal cells. P-values were calculated using unpaired, two-sided Student's *t* tests.

Online supplemental material

Fig. S1 shows Rho1 protein depletion in Rho1-RNAi–expressing tissue and a rescue of the Rho1-RNAi phenotype with Rho1 expression. Fig. S2 shows enhancement of the Rho1-RNAi phenotype by removal of a genomic copy of Rho1, Rho1 depletion disrupting AJs but not SJs, single-cell DE-cadherin–null clones with disrupted AJs, and Rok- and Rho1-null clones with decreased phospho-MLC immunofluorescence levels. Fig. S3 shows Dia LOF clones with a temperature shift and Daam LOF and CA clones. Fig. S4 shows Rab5-RNAi expression in Rho1-null clones, clones expressing Rab5-DN, Rab5-RNAi, or Rab5-CA alone, and DE-cadherin and Rab5-GFP localization in control and Rho1-RNAi–expressing pupal eyes. Fig. S5 shows F-actin disruption in Chickadee-null clones, PKN-RNAi expression in the pupal eye, and Crumbs localization in Rho1- or DE-cadherin–null clones. Video 1 shows time-lapse imaging of AJs in control pupal eye between 20 and 28 h APF. Videos 2 and 3 show time-lapse imaging of AJs in pupal eyes expressing Rho1-RNAi 20–23 h APF and 23–28 h APF, respectively. Table S1 quantifies apical areas in Rho1, Dia, and Rok LOF clones. Table S2 quantifies F-actin in Rho1, Rok, Dia, and Chickadee LOF clones. Table S3 quantifies phospho-MLC in Rho1- and Rok-null clones. Tables S4 and S5 quantify the AJ index and apical areas, respectively, in Rho1-null clones expressing various transgenes. Online supplemental material is available at http://www.jcb.org/cgi/content/full/jcb.200901029/DC1.

We thank R. Cagan for support during the initial stages of this work. We thank M. Peifer, T. Wolff, R. Karess, J. Mihály, G.-C. Chen, C. Doe, D. Ready, U. Tepass, S. Wasserman, M. González-Gaitán, the Vienna Drosophila RNAi Center, the National Institute of Genetics, the Bloomington Drosophila Stock Center, and the Developmental Studies Hybridoma Bank for reagents. We also thank D. Larson for help with live imaging and C. Micchelli for helpful discussions.

This work was supported by National Institutes of Health grants CA85839 and GM080673 to G.D. Longmore.

Submitted: 8 January 2009
Accepted: 12 May 2009

References

Adams, C.L., Y.T. Chen, S.J. Smith, and W.J. Nelson. 1998. Mechanisms of epithelial cell-cell adhesion and cell compaction revealed by high-resolution tracking of E-cadherin-green fluorescent protein. *J. Cell Biol.* 142:1105–1119.

Bao, S., and R. Cagan. 2005. Preferential adhesion mediated by Hibris and Roughest regulates morphogenesis and patterning in the *Drosophila* eye. *Dev. Cell*. 8:925–935.

Bao, S., and R. Cagan. 2006. Fast cloning inverted repeats for RNA interference. *RNA*. 12:2020–2024.

Bishop, A.L., and A. Hall. 2000. Rho GTPases and their effector proteins. *Biochem. J.* 348:241–255.

Braga, V.M., L.M. Machesky, A. Hall, and N.A. Hotchin. 1997. The small GTPases Rho and Rac are required for the establishment of cadherin-dependent cell-cell contacts. *J. Cell Biol.* 137:1421–1431.

Cagan, R.L., and D.F. Ready. 1989. The emergence of order in the *Drosophila* pupal retina. *Dev. Biol.* 136:346–362.

Capaldo, C.T., and I.G. Macara. 2007. Depletion of E-cadherin disrupts establishment but not maintenance of cell junctions in Madin-Darby canine kidney epithelial cells. *Mol. Biol. Cell*. 18:189–200.

Carramusa, L., C. Ballestrem, Y. Zilberman, and A.D. Bershadsky. 2007. Mammalian diaphanous-related formin Dia1 controls the organization of E-cadherin-mediated cell-cell junctions. *J. Cell Sci.* 120:3870–3882.

Conti, M.A., and R.S. Adelstein. 2008. Nonmuscle myosin II moves in new directions. *J. Cell Sci.* 121:11–18.

Corrigall, D., R.F. Walther, L. Rodriguez, P. Fichelson, and F. Pichaud. 2007. Hedgehog signaling is a principal inducer of Myosin-II-driven cell ingression in *Drosophila* epithelia. *Dev. Cell*. 13:730–742.

D'Souza-Schorey, C. 2005. Disassembling adherens junctions: breaking up is hard to do. *Trends Cell Biol.* 15:19–26.

Eaton, B.A., and G.W. Davis. 2005. LIM Kinase1 controls synaptic stability downstream of the type II BMP receptor. *Neuron*. 47:695–708.

Furuse, M., and S. Tsukita. 2006. Claudins in occluding junctions of humans and flies. *Trends Cell Biol.* 16:181–188.

Georgiou, M., E. Marinari, J. Burden, and B. Baum. 2008. Cdc42, Par6, and aPKC regulate Arp2/3-mediated endocytosis to control local adherens junction stability. *Curr. Biol.* 18:1631–1638.

Gumbiner, B., B. Stevenson, and A. Grimaldi. 1988. The role of the cell adhesion molecule uvomorulin in the formation and maintenance of the epithelial junctional complex. *J. Cell Biol.* 107:1575–1587.

Gumbiner, B.M. 2005. Regulation of cadherin-mediated adhesion in morphogenesis. *Nat. Rev. Mol. Cell Biol.* 6:622–634.

Habas, R., Y. Kato, and X. He. 2001. Wnt/Frizzled activation of Rho regulates vertebrate gastrulation and requires a novel Formin homology protein Daam1. *Cell*. 107:843–854.

Hakem, A., O. Sanchez-Sweatman, A. You-Ten, G. Duncan, A. Wakeham, R. Khokha, and T.W. Mak. 2005. RhoC is dispensable for embryogenesis and tumor initiation but essential for metastasis. *Genes Dev.* 19:1974–1979.

Harden, N., M. Ricos, Y.M. Ong, W. Chia, and L. Lim. 1999. Participation of small GTPases in dorsal closure of the *Drosophila* embryo: distinct roles for Rho subfamily proteins in epithelial morphogenesis. *J. Cell Sci.* 112:273–284.

Harris, K.P., and U. Tepass. 2008. Cdc42 and Par proteins stabilize dynamic adherens junctions in the *Drosophila* neuroectoderm through regulation of apical endocytosis. *J. Cell Biol.* 183:1129–1143.

Hollande, F., A. Shulkes, and G.S. Baldwin. 2005. Signaling the junctions in gut epithelium. *Sci. STKE*. doi:10.1126/stke.2772005pe13.

Homem, C.C., and M. Peifer. 2008. Diaphanous regulates myosin and adherens junctions to control cell contractility and protrusive behavior during morphogenesis. *Development*. 135:1005–1018.

Ito, K., W. Awano, K. Suzuki, Y. Hiromi, and D. Yamamoto. 1997. The *Drosophila* mushroom body is a quadruple structure of clonal units each of which contains a virtually identical set of neurones and glial cells. *Development*. 124:761–771.

Jacinto, A., S. Woolner, and P. Martin. 2002. Dynamic analysis of dorsal closure in *Drosophila*: from genetics to cell biology. *Dev. Cell*. 3:9–19.

Johndrow, J.E., C.R. Magie, and S.M. Parkhurst. 2004. Rho GTPase function in flies: insights from a developmental and organismal perspective. *Biochem. Cell Biol.* 82:643–657.

Kobielak, A., H.A. Pasolli, and E. Fuchs. 2004. Mammalian formin-1 participates in adherens junctions and polymerization of linear actin cables. *Nat. Cell Biol.* 6:21–30.

Larson, D.E., Z. Liberman, and R.L. Cagan. 2008. Cellular behavior in the developing *Drosophila* pupal retina. *Mech. Dev.* 125:223–232.

Le Borgne, R., and F. Schweisguth. 2003. Unequal segregation of Neuralized biases Notch activation during asymmetric cell division. *Dev. Cell*. 5:139–148.

Lee, T., and L. Luo. 1999. Mosaic analysis with a repressible cell marker for studies of gene function in neuronal morphogenesis. *Neuron*. 22:451–461.

Leibfried, A., R. Fricke, M.J. Morgan, S. Bogdan, and Y. Bellaiche. 2008. *Drosophila* Cip4 and WASp define a branch of the Cdc42-Par6-aPKC pathway regulating E-cadherin endocytosis. *Curr. Biol.* 18:1639–1648.

Liu, A.X., N. Rane, J.P. Liu, and G.C. Prendergast. 2001. RhoB is dispensable for mouse development, but it modifies susceptibility to tumor formation as well as cell adhesion and growth factor signaling in transformed cells. *Mol. Cell. Biol.* 21:6906–6912.

Matusek, T., A. Djiane, F. Jankovics, D. Brunner, M. Mlodzik, and J. Mihaly. 2006. The *Drosophila* formin DAAM regulates the tracheal cuticle pattern through organizing the actin cytoskeleton. *Development*. 133:957–966.

Mukai, H. 2003. The structure and function of PKN, a protein kinase having a catalytic domain homologous to that of PKC. *J. Biochem.* 133:17–27.

Downloaded from http://rupress.org/jcb/article-pdf/185/6/1111/1899046/jcb_200901029.pdf by guest on 05 December 2025

Mulinari, S., M.P. Padash Barmchi, and U. Häcker. 2008. DRhoGEF2 and diaphanous regulate contractile force during segmental groove morphogenesis in the drosophila embryo. *Mol. Biol. Cell*. 19:1883–1892.

Niessen, C.M. 2007. Tight junctions/adherens junctions: basic structure and function. *J. Invest. Dermatol.* 127:2525–2532.

Ridley, A.J. 2006. Rho GTPases and actin dynamics in membrane protrusions and vesicle trafficking. *Trends Cell Biol.* 16:522–529.

Sahai, E., and C.J. Marshall. 2002. ROCK and Dia have opposing effects on adherens junctions downstream of Rho. *Nat. Cell Biol.* 4:408–415.

Somogyi, K., and P. Rorth. 2004. Evidence for tension-based regulation of *Drosophila* MAL and SRF during invasive cell migration. *Dev. Cell*. 7:85–93.

Symons, M., and N. Rusk. 2003. Control of vesicular trafficking by Rho GTPases. *Curr. Biol.* 13:R409–R418.

Takaishi, K., T. Sasaki, H. Kotani, H. Nishioka, and Y. Takai. 1997. Regulation of cell-cell adhesion by rac and rho small G proteins in MDCK cells. *J. Cell Biol.* 139:1047–1059.

Tepass, U., and K.P. Harris. 2007. Adherens junctions in *Drosophila* retinal morphogenesis. *Trends Cell Biol.* 17:26–35.

Vega, F.M., and A.J. Ridley. 2007. SnapShot: Rho family GTPases. *Cell*. 129:1430.

Wang, L., and Y. Zheng. 2007. Cell type-specific functions of Rho GTPases revealed by gene targeting in mice. *Trends Cell Biol.* 17:58–64.

Wennerberg, K., and C.J. Der. 2004. Rho-family GTPases: it's not only Rac and Rho (and I like it). *J. Cell Sci.* 117:1301–1312.

Wheeler, A.P., and A.J. Ridley. 2004. Why three Rho proteins? RhoA, RhoB, RhoC, and cell motility. *Exp. Cell Res.* 301:43–49.

Xu, T., and G.M. Rubin. 1993. Analysis of genetic mosaics in developing and adult *Drosophila* tissues. *Development*. 117:1223–1237.

Yamada, S., and W.J. Nelson. 2007. Localized zones of Rho and Rac activities drive initiation and expansion of epithelial cell–cell adhesion. *J. Cell Biol.* 178:517–527.

Yap, A.S., M.S. Crampton, and J. Hardin. 2007. Making and breaking contacts: the cellular biology of cadherin regulation. *Curr. Opin. Cell Biol.* 19:508–514.

Zhang, J., K.L. Schulze, P.R. Hiesinger, K. Suyama, S. Wang, M. Fish, M. Acar, R.A. Hoskins, H.J. Bellen, and M.P. Scott. 2007. Thirty-one flavors of *Drosophila* rab proteins. *Genetics*. 176:1307–1322.

Downloaded from http://rupress.org/jcb/article-pdf/185/6/1111/1899046/jcb_200901029.pdf by guest on 05 December 2025